Synthesis of Highly Crystalline and Monodisperse Maghemite Nanocrystallites without a Size-Selection Process

Taeghwan Hyeon,* Su Seong Lee, Jongnam Park, Yunhee Chung, and Hyon Bin Na

Contribution from the School of Chemical Engineering and Institute of Chemical Processes, Seoul National University, Seoul 151-744, Korea

Received August 10, 2001

Abstract: The synthesis of highly crystalline and monodisperse γ-Fe_2O_3 nanocrystallites is reported. High-temperature (300 °C) aging of iron−oleic acid metal complex, which was prepared by the thermal decomposition of iron pentacarbonyl in the presence of oleic acid at 100 °C, was found to generate monodisperse iron nanoparticles. The resulting iron nanoparticles were transformed to monodisperse γ-Fe_2O_3 nanocrystallites by controlled oxidation by using trimethylamine oxide as a mild oxidant. Particle size can be varied from 4 to 16 nm by controlling the experimental parameters. Transmission electron microscopic images of the particles showed 2-dimensional and 3-dimensional assembly of particles, demonstrating the uniformity of these nanoparticles. Electron diffraction, X-ray diffraction, and high-resolution transmission electron microscopic (TEM) images of the nanoparticles showed the highly crystalline nature of the γ-Fe_2O_3 structures. Monodisperse γ-Fe_2O_3 nanocrystallites with a particle size of 13 nm also can be generated from the direct oxidation of iron pentacarbonyl in the presence of oleic acid with trimethylamine oxide as an oxidant.

Introduction

The development of uniform nanometer sized particles has been intensively pursued because of their technological and fundamental scientific importance.[1] These nanoparticular materials often exhibit very interesting electrical, optical, magnetic, and chemical properties, which cannot be achieved by their bulk counterparts.[2] So far, the majority of nanoparticle research has been focused upon II−VI semiconductors and noble metals. Comparatively little work has been conducted upon the fabrication of uniform oxide nanoparticles despite their many important technological applications.[3] The fabrication of patterned media arrays of discrete single domain magnetic nanoparticles is very important for their potential applications in multi-terabit/in^2 magnetic memory devices.[4] Such magnetic nanoparticles could also find applications in ferrofluids, refrigeration systems, medical imaging, drug targeting, and catalysis.[5] The syntheses of several uniform-sized magnetic metal nanoparticles have been reported.[6] However, relatively little work has been done on the fabrication of monodispersed and crystalline magnetic oxide nanoparticles. Several magnetic oxide nanoparticles including γ-Fe_2O_3 and magnetite have been synthesized by using microemulsion and other methods.[7] However, particle size uniformity and the crystallinity of these nanoparticles are comparatively poor. Although the syntheses of relatively uniform maghemite and magnetite nanoparticles have been recently reported, exhaustive size selection procedures were necessary.[8] Here we report upon a novel non-hydrolytic synthetic method of fabricating highly crystalline and monodisperse γ-Fe_2O_3 nanocrystalline particles without a size selection process, which allows the production of selected particle sizes from 4 to 16 nm.

Experimental Section

Synthesis of γ-Fe_2O_3 Nanocrystallites through the Oxidation of Iron Nanoparticles. To prepare monodispersed iron nanoparticles, 0.2 mL of $Fe(CO)_5$ (1.52 mmol) was added to a mixture containing 10 mL of octyl ether and 1.28 g of oleic acid (4.56 mmol) at 100 °C. The resulting mixture was heated to reflux and kept at that temperature for 1 h. During this process, the initial orange color of the solution gradually

(1) (a) Alivisatos, A. P. *Science* **1996**, *271*, 933. (b) Weller, H. *Angew. Chem., Int. Ed. Engl.* **1993**, *32*, 41. (c) Schmid, G., Ed. *Clusters and Colloids*; VCH Press: New York, 1994.

(2) (a) Ashoori, R. C. *Nature* **1996**, *379*, 413. (b) Billas, I. M. L.; Chatelain, A.; de Heer, W. A. *Science* **1994**, *265*, 1682. (c) Murray, C. B.; Norris, D. J.; Bawendi, M. G. *J. Am. Chem. Soc.* **1993**, *115*, 8706. (d) Vossmeyer, T.; Katsikas, L.; Giersig, M.; Popovic, I. G.; Diesner, K.; Chemseddine, A.; Eychmüller; Weller, H. *J. Phys. Chem.* **1994**, *98*, 7665. (e) Tolbert, S. H.; Alivisatos, A. P. *Science* **1994**, *265*, 373.

(3) (a) Trentler, T. J.; Denler, T. E.; Bertone, J. F.; Agrwal, A.; Colvin, V. L. *J. Am. Chem. Soc.* **1999**, *121*, 1613. (b) Liu, C.; Zou, B.; Rondinone, A. J.; Zhang, Z. J. *J. Am. Chem. Soc.* **2001**, *123*, 4344.

(4) (a) Awschalom, D. D.; DiVicenzo, D. P. *Phys. Today* **1995**, *4*, 43. (b) Leslie-Pelecky, D. L.; Rieke, R. D. *Chem. Mater.* **1996**, *8*, 1770. (c) Raj, K.; Moskowitz, R. *J. Magn. Magn. Mater.* **1990**, *85*, 233. (d) Speliotis, D. E. *J. Magn. Magn. Mater.* **1999**, *193*, 29.

(5) (a) Cornell, R. M.; Schwertmann, U. *The iron oxides*; VCH: Weinheim, Germany, 1996. (b) Fertman, V. E. *Magnetic Fluids Guidebook: Properties and Applications*; Hemisphere Publishing Co.: New York, 1990. (c) Berkovsky, B. M.; Medvedev, V. F.; Krakov, M. S. *Magnetic Fluids: Engineering Applications*; Oxford University Press: Oxford, 1993. (d) Ziolo, R. F.; Giannelis, E. P.; Weinstein, B. A.; O'Horo, M. P.; Ganguly, B. N.; Mehrotra, V.; Russel, M. W.; Huffman, D. R. *Science* **1992**, *257*, 219.

(6) (a) Park, S.-J.; Kim, S.; Lee, S.; Khim, Z. G.; Char, K.; Hyeon, T. *J. Am. Chem. Soc.* **2000**, *122*, 8581. (b) Puntes, A. F.; Krishnan, K. M.; Alivisatos, A. P. *Science* **2001**, *291*, 2115. (c) Sun, S.; Murray, C. B. *J. Appl. Phys.* **1999**, *85*, 4325. (d) Sun, S.; Murray, C. B.; Weller, D.; Folks, L.; Moser, A. *Science* **2000**, *287*, 1989. (e) Suslick, K. S.; Fang, M.; Hyeon, T. *J. Am. Chem. Soc.* **1996**, *118*, 11960.

(7) (a) Feltin, N.; Pileni, M. P. *Langmuir* **1997**, *13*, 3927. (b) Rondinone, A. J.; Samia, A. C. S.; Zhang, Z. J. *J. Phys. Chem.* **1999**, *103*, 6876. (c) Kang, Y. S.; Risbud, S.; Rabolt, J. F.; Stroeve, P. *Chem. Mater.* **1996**, *8*, 2209. (d) Easom, K. A.; Klabunde, K. J.; Sorensen, C. M. *Polyhedron* **1994**, *13*, 1197. (e) Tamura, H.; Matijevic, E. *J. Colloid Interface Sci.* **1982**, *90*, 100. (f) Benton, M. D.; van Wonterghem, J.; Mørup, S.; Thölén, A.; Koch, C. J. W. *Philos. Mag. B* **1989**, *60*, 169. (g) Hong, C.-Y.; Jang, I. J.; Horng, H. E.; Hsu, C. J.; Yao, Y. D.; Yang, H. C. *J. Appl. Phys.* **1997**, *81*, 4275.

(8) (a) Rockenberger, J.; Scher, E. C.; Alivisatos, A. P. *J. Am. Chem. Soc.* **1999**, *121*, 11595. (b) Fried, T.; Shemer, G.; Markovich, G. *Adv. Mater.* **2001**, *13*, 1158.

10.1021/ja016812s CCC: $20.00
Published on Web 11/29/2001

changed to black. The resulting black solution was cooled to room temperature and 0.34 g of dehydrated $(CH_3)_3NO$ (4.56 mmol) was added. The mixture was then heated to 130 °C under an argon atmosphere and maintained at this temperature for 2 h, whereupon it formed a brown solution. The reaction temperature was slowly increased to reflux and the reflux continued for 1 h; the color of the solution gradually turned from brown to black. The solution was then cooled to room temperature, and ethanol was added to yield a black precipitate, which was then separated by centrifuging. The resulting black powder can be easily re-dispersed in hydrocarbon solvents, such as hexane, octane, and toluene.

Synthesis of 13 nm Sized γ-Fe_2O_3 Nanocrystallites through the Oxidative Decomposition of Iron Pentacarbonyl. $Fe(CO)_5$ (0.2 mL, 1.52 mmol) was injected into a solution containing 0.91 g of lauric acid (4.56 mmol), 7 mL of octyl ether, and 0.57 g of $(CH_3)_3NO$ (7.60 mmol) at 100 °C in an argon atmosphere, with vigorous stirring. As soon as $Fe(CO)_5$ was injected into the mixture, the temperature rose to 120 °C and the solution became dark-red, which indicated the successful oxidation of $Fe(CO)_5$. The reaction mixture was then stirred for 1 h at 120 °C, and the solution was slowly heated to reflux. The solution color gradually became black, indicating that nanoparticles were being formed. After refluxing for 1 h, the solution was cooled to room temperature, and a black precipitate was obtained upon adding excess ethanol and centrifuging. The precipitate can be easily redispersed in octane or toluene.

Characterization of Materials. Nanocrystallites were characterized by low- and high-resolution TEM, electron diffraction, and X-ray diffraction. Low-resolution transmission electron micrographs were obtained on a JEOL EM-2000 EX II microscope. High-resolution transmission electron micrographs were taken on a JEOL JEM-3000F microscope. X-ray diffraction pattern was obtained with a Rigaku D/Max-3C diffractometer equipped with a rotating anode and a Cu Kα radiation source ($\lambda = 0.15418$ nm).

Results and Discussion

Two different approaches were applied in the synthesis. In the first method, monodisperse iron nanoparticles were first generated and were further oxidized to iron oxide. In the second approach, $Fe(CO)_5$ was directly injected into a solution containing both the surfactant and trimethylamine oxide. In both approaches, monodisperse iron oxide nanocrystallites were directly obtained without a further size selection process; however, the first method allowed better control of particle size and reproducibility. By varying the experimental conditions, we were able to get γ-Fe_2O_3 nanocrystallites with different particle sizes. The nanoparticles obtained were characterized by low-resolution and high-resolution TEM, electron diffraction, X-ray powder diffraction, X-ray photoelectron spectroscopy, and Raman spectroscopy.

In the following, a typical fabrication of iron oxide nanocrystallites with a particle diameter of 11 nm through the first synthetic method is described. At first, the iron oleate complex was prepared by reacting $Fe(CO)_5$ and oleic acid with a 1:3 molar ratio at 100 °C. The UV−visible absorption spectrum of the metal complex revealed a single intense peak at 330 nm (Supporting Information), and the FT-IR spectrum of the complex exhibited no CO stretching peak. These spectroscopic data and the Mössbauer spectroscopic results on the decomposition of iron pentacarbonyl at 120 °C reported by Wonterghem and co-workers[9] demonstrate that the iron(II) complex seemed to be produced. However, the exact structure of the complex was not elucidated. Iron nanoparticles were then generated by aging iron complex at 300 °C. The TEM image of the iron nanoparticles (Supporting Information) revealed that nanoparticles are monodisperse. The electron diffraction pattern showed that the nanoparticles are nearly amorphous. The XRD pattern of the sample after being heat treated under argon atmosphere at 500 °C revealed a bcc α-iron structure. These iron nanoparticles were then transformed into γ-Fe_2O_3 nanocrystallites by oxidizing them at 300 °C with a mild oxidant, trimethylamine oxide ($(CH_3)_3NO$). The TEM image (Figure 1) showed that monodisperse nanoparticles of 11 nm diameter were arranged in a 2-dimensional hexagonal closed packed way, demonstrating the uniformity of the particle size. The high-resolution transmission electron micrograph (HRTEM) shown in Figure 2 illustrates the highly crystalline nature of the nanoparticles. The electron diffraction pattern exhibited a maghemite (γ-Fe_2O_3) structure (Figure 3).

The X-ray powder diffraction pattern of the material also proved its highly crystalline nature and the peaks matched well with standard γ-Fe_2O_3 reflections (Figure 4). The XRD peaks of the nanocrystallites were compared with those of standard maghemite and magnetite data (Supporting Information). In the X-ray photoelectron spectrum, the positions of the $Fe(2p_{3/2})$ and

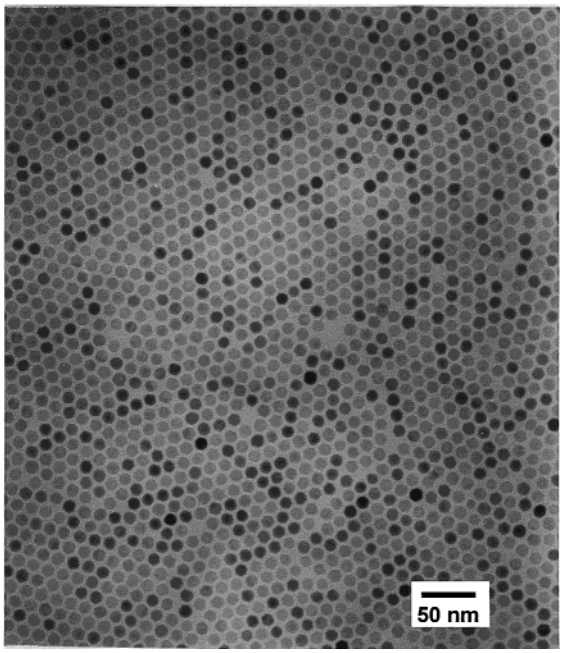

Figure 1. TEM image of a two-dimensional hexagonal assembly of 11 nm γ-Fe_2O_3 nanocrystallites.

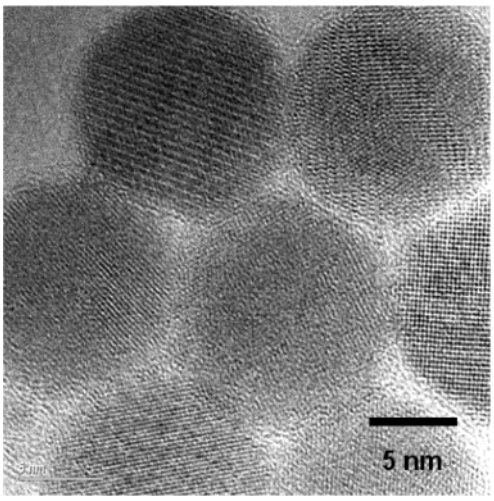

Figure 2. High-resolution TEM image of 2D hexagonally close-packed 11 nm γ-Fe_2O_3 nanocrystallites.

(9) (a) van Wonterghem, J.; Mørup, S.; Charles, S. W.; Wells, S. *J. Colloid Interface Sci.* **1988**, *121*, 558. (b) van Wonterghem, J.; Mørup, S.; Charles, S. W.; Wells, S.; Villadsen, J. *Phys. Rev. Lett.* **1985**, *55*, 410.

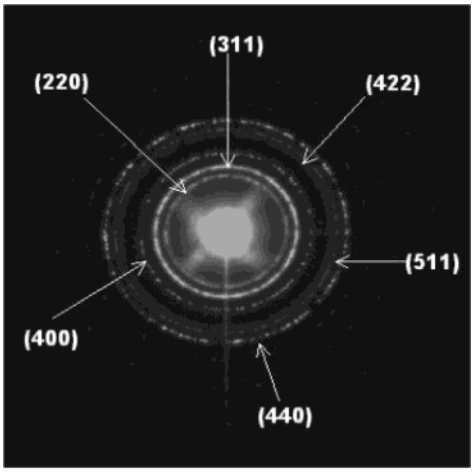

Figure 3. Electron diffraction pattern of 11 nm γ-Fe_2O_3 nanocrystallites.

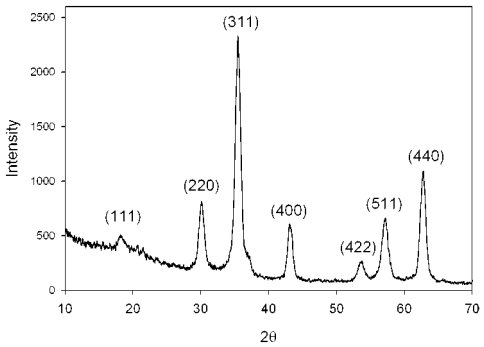

Figure 4. X-ray diffraction pattern of 11 nm γ-Fe_2O_3 nanocrystallites.

Fe($2p_{1/2}$) peaks are 711.3 and 724.4 eV, which are in good agreement with the values reported for γ-Fe_2O_3 in the literature (Supporting Information).[10] The Raman spectrum, which was often applied as a tool to differentiate between maghemite and magnetite, matched well with the reported maghemite spectrum (Supporting Information).[11] By manipulating the TEM sample preparation condition, we could obtain a 3-dimensional close-packed superlattice assembly (Figure 5).

When the starting reaction mixture containing 1:1 and 1:2 molar ratios of $Fe(CO)_5$ and oleic acid were applied in the synthesis, γ-Fe_2O_3 nanocrystallites with particle sizes of 4 and 7 nm were obtained, respectively. The low-resolution and high-resolution TEM image of the 7 nm sized nanocrystallites are shown in Figure 6. The low-resolution TEM images of γ-Fe_2O_3 nanocrystallites with a particle diameter of 4 nm are shown in Figure 7.

To produce bigger nanocrystallites of >11 nm, a reaction mixture with a 1:4 molar ratio of $Fe(CO)_5$ and oleic acid was applied in the synthesis. The particle size of the resulting nanocrystallites was, however, still around 11 nm. However, we could get iron nanocrystallites with particle sizes bigger than 11 nm by adding more iron oleate complex into the previously prepared 11 nm sized iron nanocrystallites, followed by aging at 300 °C. The resulting bigger iron nanocrystallites were later oxidized to get monodisperse γ-Fe_2O_3 nanocrystallites through a similar procedure as described above. Through this synthetic procedure, we could tune the particle size of the nanocrystallites from 11 to 16 nm. The TEM images of the γ-Fe_2O_3 nanocrystallites with particle sizes of 16 nm through the synthetic procedure are shown in Figure 8.

We have also used a second synthetic procedure, employing the direct oxidative decomposition of $Fe(CO)_5$ in the presence of trimethylamine oxide and a surfactant, to fabricate uniform γ-Fe_2O_3 nanocrystallites. The low- and high-resolution TEM images of γ-Fe_2O_3 nanocrystallites (Figure 9) demonstrated that

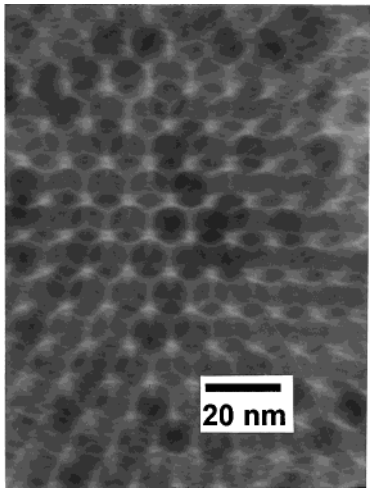

Figure 5. TEM image of a three-dimensional superlattice of 11 nm γ-Fe_2O_3 nanocrystallites.

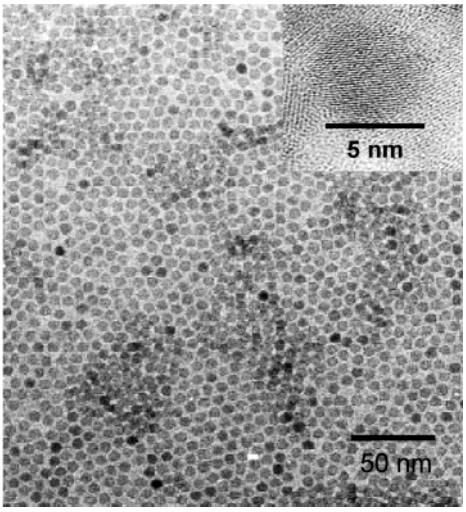

Figure 6. Low-resolution TEM image and high-resolution TEM image of a single nanocrystallite (inset) of 7 nm γ-Fe_2O_3 nanocrystallites.

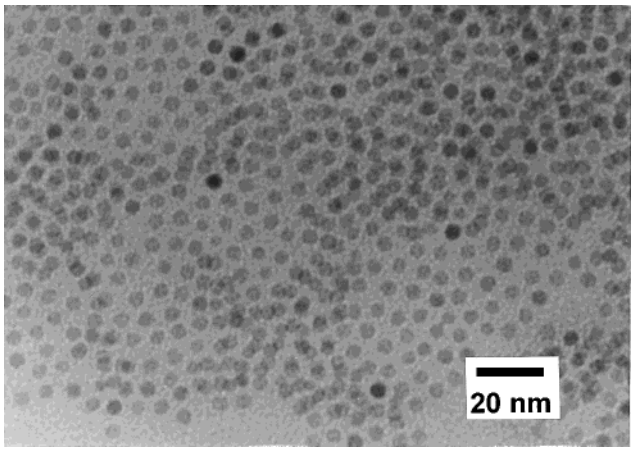

Figure 7. TEM image of 4 nm γ-Fe_2O_3 nanocrystallites.

(10) (a) Sohn, B. H.; Cohen, R. E. *Chem. Mater.* **1997**, *9*, 264. (b) Graat, P.; Somers, M. A. J. *Surf. Interface Anal.* **1998**, *26*, 773.

(11) (a) de Faria, D. L. A.; Silva, S. V.; de Oliverira, M. T. *J. Raman Spectrosc.* **1997**, *28*, 873. (b) Pascal, C.; Pascal, J. L.; Favier, F.; Moubtassim, M. L. E.; Payen, C. *Chem. Mater.* **1999**, *11*, 141.

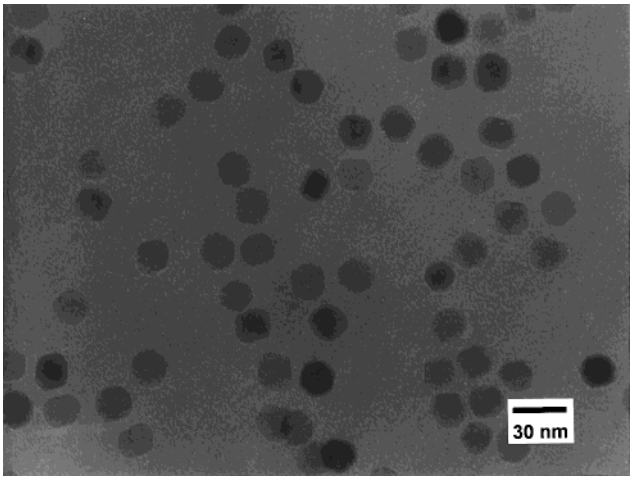

Figure 8. TEM image of 16 nm γ-Fe_2O_3 nanocrystallites.

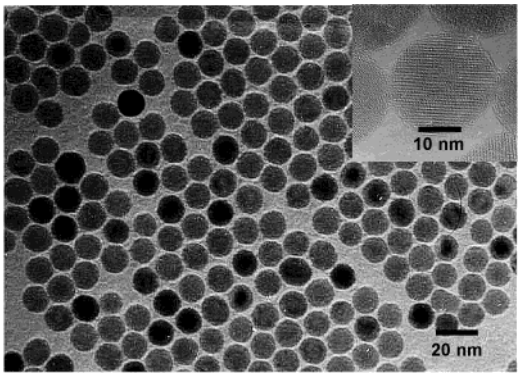

Figure 9. Low-resolution and high-resolution TEM image of a single nanocrystallite (inset) of 13 nm γ-Fe_2O_3 nanocrystallites.

the particle size is very uniform and highly crystalline, with a diameter of 13 nm.

Preliminary magnetic measurements were performed on the γ-Fe_2O_3 nanocrystallites with use of a superconducting quantum interference device (SQUID). The temperature dependence of the magnetization was measured with use of zero-field cooling (ZFC) and field cooling (FC) procedures in an applied magnetic field of 100 Oe between 5 and 300 K. The plot of temperature versus magnetization for 4, 13, and 16 nm γ-Fe_2O_3 nanocrystallites with zero-field cooling (ZFC) is presented in Figure 10. The blocking temperatures of the γ-Fe_2O_3 nanocrystallites with particle diameters of 4, 13, and 16 nm were found to be 25, 185, and ~290 K, respectively. Detailed magnetic studies of the γ-Fe_2O_3 nanocrystallites are currently underway.

Conclusions

The highly crystalline and monodisperse γ-Fe_2O_3 nanocrystallites were fabricated from the controlled oxidation of uniform iron nanoparticles which were generated from the thermal decomposition of iron complex. The synthetic procedures developed in the present study offer several very important advantageous features for the fabrication of oxide nanoparticles. First, they allow highly crystalline and monodisperse nanoparticles to be obtained directly without a further size-selection process. Second, particle size can be easily and reproducibly altered by changing the experimental parameters. Third, the nanocrystallites can be easily dispersed in many hydrocarbons without particle aggregation. In addition, the yield of the current process is over 80% and the indications are that scale-up can be achieved relatively easily.

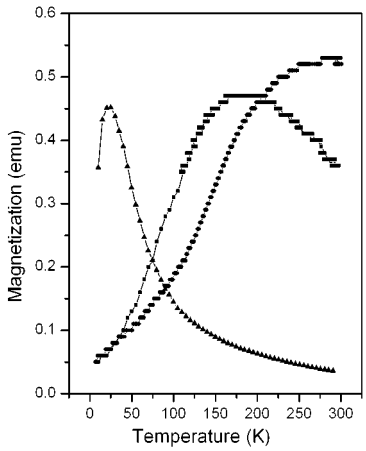

Figure 10. Magnetization versus temperature for 4 (triangles), 13 (squares) , and 16 nm (circles) γ-Fe_2O_3 nanocrystallites with zero-field cooling at the applied magnetic field of 100 Oe. The magnetic studies were conducted with a Quantum Design MPMS SQUID magnetometer.

Acknowledgment. We are grateful to the Korea Institute of Science and Technology (KIST) for financial support. We also would like to thank Prof. Kwan Kim and Dr. Sang Woo Han for the Raman spectroscopic studies, Prof. Zheong G. Khim, Suyoun Lee, and Joonsung Lee for the magnetic studies, and Mee Jeong Kang for the TEM studies.

Supporting Information Available: UV−visible absorption spectrum of iron oleate complex, TEM image of 11 nm iron nanoparticles, XRD pattern of 11 nm iron nanoparticles after heating under Ar at 500 °C, a table showing the comparison of *d* spacing values of the synthesized iron oxide nanocrystallites with standard JCPDS γ-Fe_2O_3 and Fe_3O_4 data, Raman spectrum of 11 nm γ-Fe_2O_3, X-ray photoelectron spectrum of 11 nm γ-Fe_2O_3, plots of magnetization versus temperature of 4, 13, and 16 nm γ-Fe_2O_3 with field cooling and zero-field cooling at the applied magnetic field of 100 Oe (PDF). This material is available free of charge via the Internet at http://pubs.acs.org.

JA016812S